Contrib. Astron. Obs. Skalnaté Pleso **53/3**, 163 – 175, (2023)
https://doi.org/10.31577/caosp.2023.53.3.163

Data quality assurance for atmospheric probing and modeling: characterization of Belgrade Raman lidar station

Z. Mijić[1], **L. Ilić**[1,2] **and M. Kuzmanoski**[1]

[1] *Institute of Physics Belgrade, Pregrevica 118, 11080 Belgrade, Serbia, (E-mail: zoran.mijic@ipb.ac.rs, maja.kuzmanoski@ipb.ac.rs)*

[2] *now at Barcelona Supercomputing Center, Plaça Eusebi Güell, 1-3, 08034 Barcelona, Spain, (E-mail: luka.ilic@ipb.ac.rs)*

Received: September 30, 2023; Accepted: November 2, 2023

Abstract. Using the lidar (Light Detection And Ranging) technique atmospheric probing and observations of atmospheric aerosol optical properties may be conducted remotely with high spatial and temporal resolution. As an EARLINET (the European Aerosol Research LIdar Network) joining lidar station, Belgrade Raman lidar system has provided aerosol profiling data for potential atmospheric and climatological studies as well as assessment of planetary boundary layer evolution and conducting dedicated measurements during airborne hazard. A comprehensive quality-assurance program and self-testing check-up tools have been developed to examine the performance and temporal stability of a lidar system. The capabilities of the Belgrade Raman lidar system, as well as its experimental characterization related to zero bin assessment, analog to photon-counting signal delay, Rayleigh-fit and telecover tests to evaluate system accuracy, are presented in this study.

Key words: Remote sensing – Atmosphere – Optical properties – Data – Quality assurance

1. Introduction

For more accurate weather predictions and a better understanding of climate change and solar influence, it is essential to quantify the impact that clouds and atmospheric aerosols play in the Earth's radiation budget (Stocker et al., 2013; Boucher et al., 2013). Depending on aerosol composition and size distribution the amount of scattered and absorbed radiation (both incoming solar and outgoing terrestrial) can differ significantly. Aerosol radiative forcing has been identified as one of the biggest climate change unknowns due to its short lifespan and high spatial and temporal variability (Stocker et al., 2013). To quantify the influence of aerosols on the climate system using an integrated approach of ground-level and airborne in-situ measurements, ground-based remote sensing, and space-based observations combined with numerical modeling are required.

Change in the incoming solar radiation flux induces disturbances in different atmospheric layers (Aplin & Harrison, 2003; Maurya et al., 2014). Several studies have investigated the effect of solar eclipse on various atmospheric properties (Ilić et al., 2018; Kolarž et al., 2005; Nymphas et al., 2009). Atmospheric lidar (Light Detection And Ranging) can be used to determine heights of planetary boundary layer (PBL) using aerosols as tracers, providing opportunity to investigate PBL evolution-based processes. Decrease in height and evolution change of PBL during a solar eclipse have been observed (Ilić et al., 2018; Amiridis et al., 2007; Kolev et al., 2005).

Lidar, an active remote sensing technique, has proved itself to be the optimal tool for profiling height-resolved atmospheric aerosol optical parameters. Various aerosol lidar techniques have been developed during the last several decades operating at one or multiple wavelengths. The lidar principle is based on laser emission of short-duration light pulses into the receiver field of view. The intensity of the light backscattered by atmospheric molecules and particles is measured versus time (through the telescope receiver, collimating optics, a bandpass filter for daylight suppression) by an appropriate detector. The signal profile is recorded by an analog-to-digital converter or by a photon-counting device and accumulated for a selected integration period spanning time intervals from seconds to minutes. In order to establish a comprehensive and quantitative statistical data base of the horizontal and vertical distribution of aerosols on the continental scale the lidar network called EARLINET (the European Aerosol Research LIdar Network) was founded in 2000 (Pappalardo et al., 2014). The development of the quality assurance strategy (Freudenthaler et al., 2018), the optimization of instruments and data processing (Wandinger et al., 2016), and the dissemination of data have contributed to significant improvement of the network towards a more sustainable observing system. With the addition of new stations EARLINET has significantly enhanced its observation capacity during the past few years. Additionally, the Single Calculus Chain (SCC) was developed eliminating inconsistencies in the optical products retrieval processes and in the signal error calculation, automating the data evaluation, and enabling near real time (NRT) data processing (D'Amico et al., 2015, 2016; Papagiannopoulos et al., 2020; Mattis et al., 2016). Such network development allowed its contribution to calibration and validation of optical products retrieval from satellite missions (Abril-Gago et al., 2022).

In this study the capabilities of the EARLINET joining Belgrade Raman lidar system combined with its experimental characterization using self-testing check-up tools developed across the network to evaluate system accuracy are presented. Aerosol optical properties retrieved from such lidar measurements can be used to evaluate aerosol satellite measurements, e.g., Earth Clouds, Aerosols and Radiation Explorer (EARTHCARE) mission (Illingworth et al., 2015), and to improve aerosol representation in climate models.

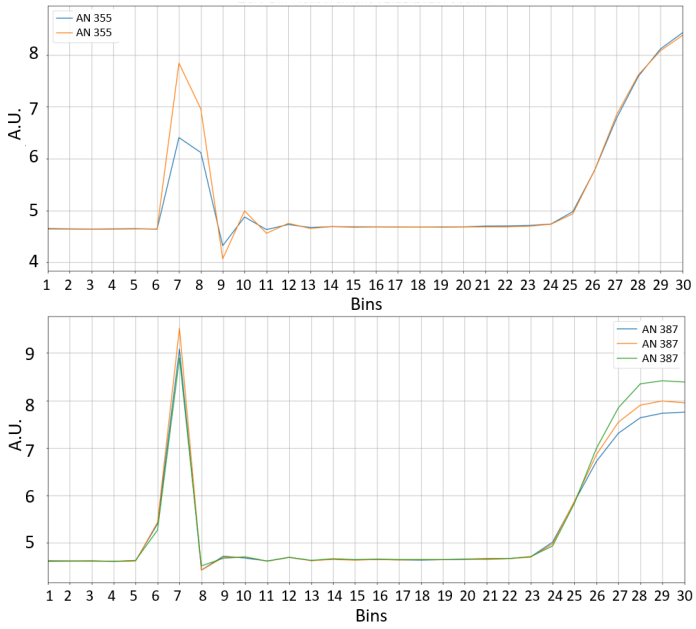

Figure 1. Zero bin assessment for elastic 355 nm (above) and Raman 387 nm (below) channels. Different color lines represent successive average signals from diffuse reflections of twenty laser shots.

2. Methodology

Raman lidar system at the Institute of Physics Belgrade (IPB), Serbia (44.860 N, 20.390 E) is bi-axial lidar system (telescope-laser axes distance is 200 mm) with combined elastic and Raman detection designed to perform continuous measurements of aerosols in the lower free troposphere (Ilić et al., 2018). Transmitter unit is based on the third harmonic frequency of a water cooled, pulsed Nd:YAG laser, emitting pulses of 65 mJ output energy at 355 nm with a 20 Hz repetition rate. In order to improve the maximum range and the precision of the system the beam expander is used to reduce the laser beam divergence (0.33 mrad) expanding the beam's diameter by 3 times. The optical receiving unit consists of two sub-units, a receiving telescope and wavelength separation unit. The optical receiver is a Cassegrain reflecting telescope with a primary mirror of 250 mm diameter and a focal length of 1250 mm. Photomultiplier tubes Hamamatsu R9880U-110 (PMT) are used to detect elastic backscatter lidar signal at 355 nm and Raman signal at 387 nm (Nitrogen vibrational scattering).

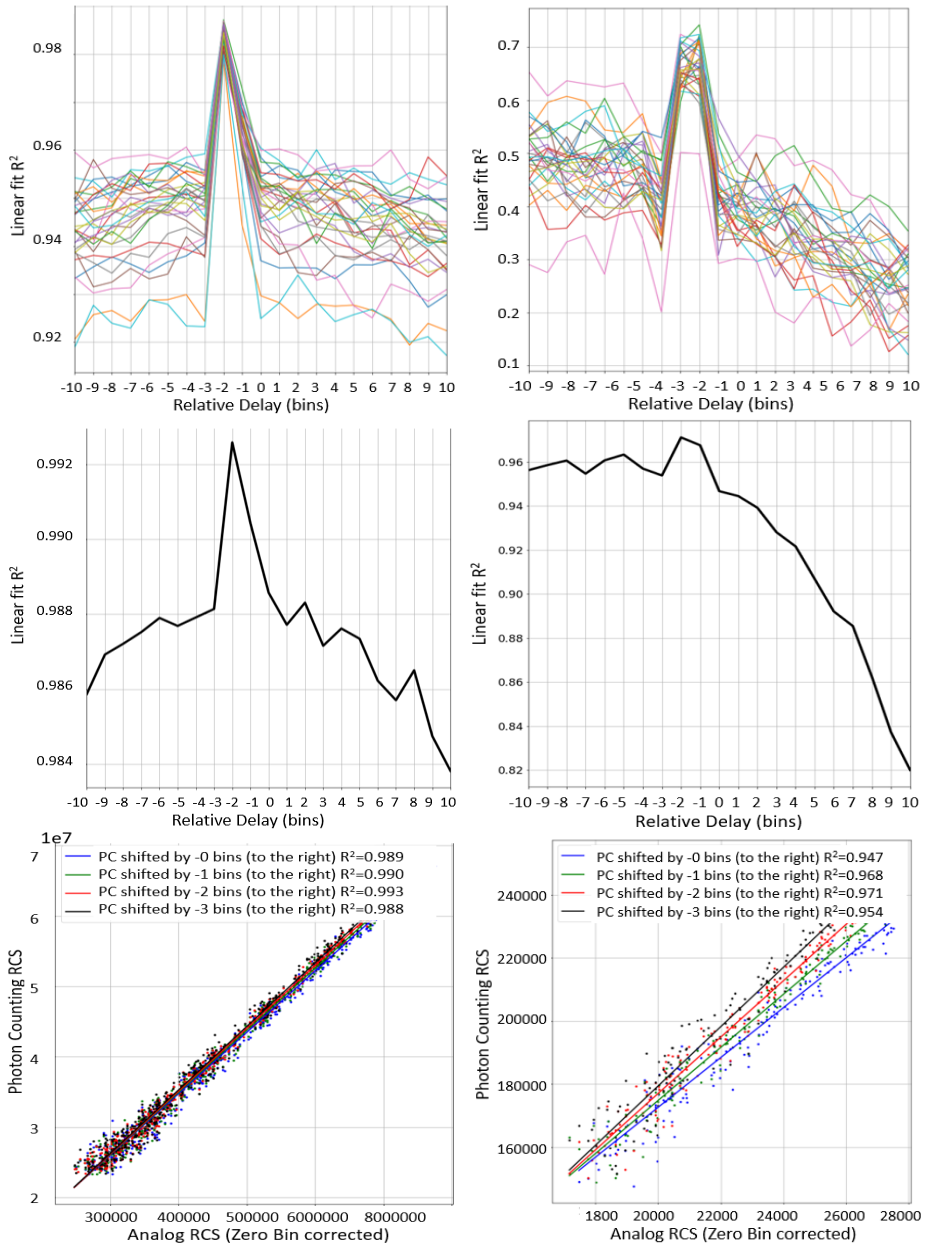

Figure 2. Analysis of the relative delay between zero-bin-corrected analog RCS and the PC RCS for 355 nm (left column) and 387 nm (right column) channels. Measurements of 30 1-minute profiles with 1200 shots each were used. A linear regression between AN and PC data was performed in the gluing region. Correlation coefficient as a function of relative delay between analog and photon counting signals (above). Correlation coefficient as a function of relative delay between analog and photon counting mean signals (center). Fit between the PC RCS and AN RCS channels (below).

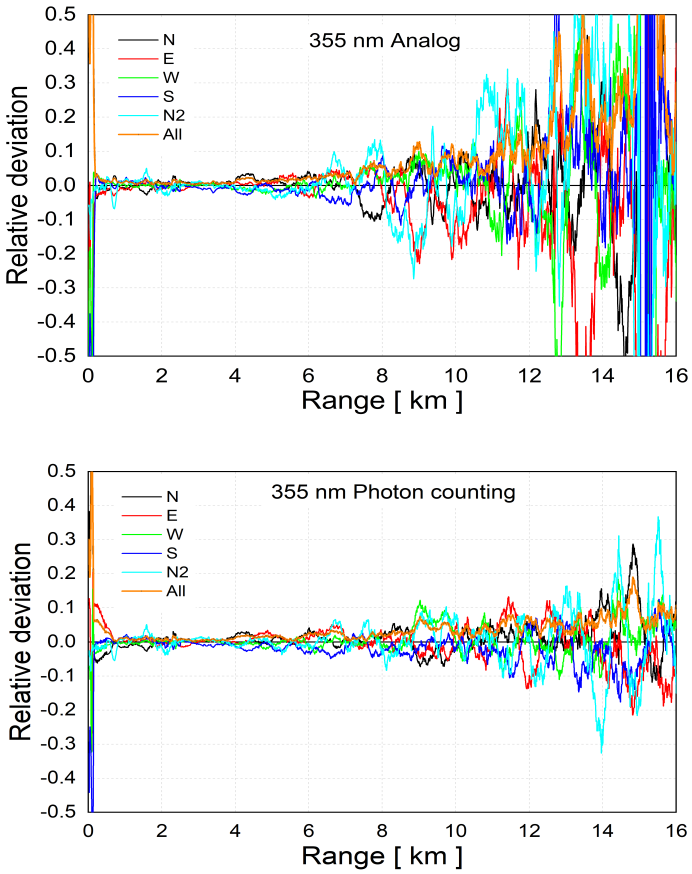

Figure 3. Relative deviations of signals collected in the four telescope sectors compared to the mean analog (above) and photon counting 355 nm signal (below), normalized in the 1500-2500 m range.

Interference filters with 0.96 nm and 0.45 nm FWHM before each PM tube are used to reduce the background noise. The detectors are operated both in the analog and photon-counting mode and the spatial raw resolution of the detected signals is 7.5 m. Averaging time of the lidar profiles is of the order of 1 min corresponding to 1200 laser shots. The Licel transient recorder is comprised of a fast transient digitizer with on board signal averaging, a discriminator for single photon detection and a multichannel scaler combined with preamplifiers for both systems. For analog detection, the signal is amplified according to the input range selected and digitized by a 12-Bit-20 MHz A/D converter. At the same time the signal part in the high frequency domain is amplified and a 250 MHz fast discriminator detects single photon events above the selected threshold voltage.

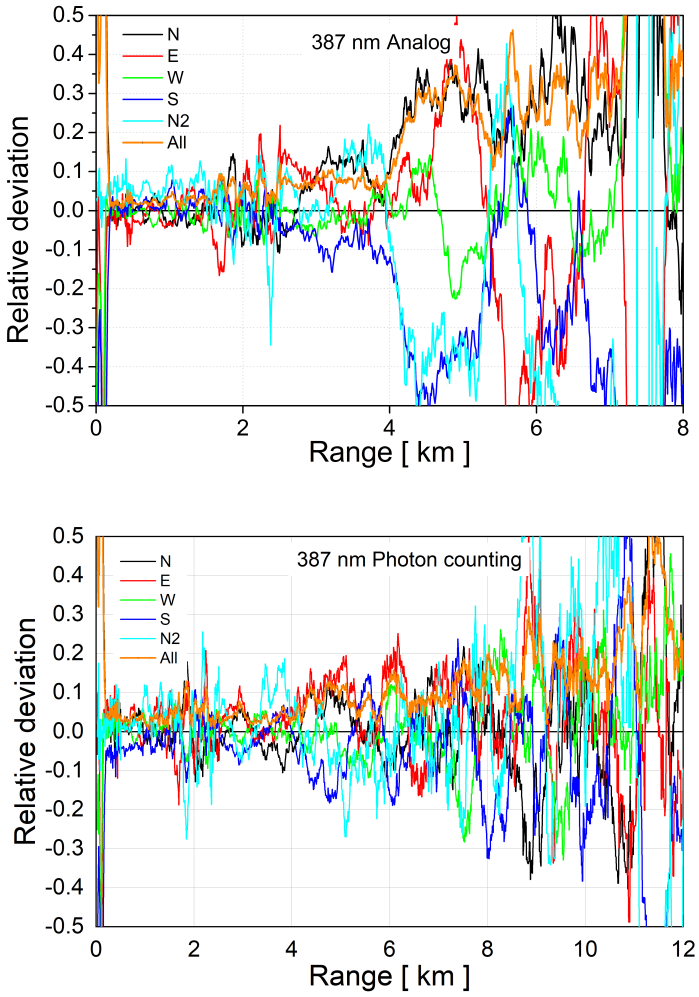

Figure 4. Relative deviations of signals collected in the four telescope sectors compared to the mean analog (above) and photon counting (below) 387 nm signal, normalized in the 1500-2500 m range.

In order to monitor and improve the quality of the lidar systems and their optical products, the quality assurance methods for both hardware and retrieval algorithms (Freudenthaler et al., 2018; D'Amico et al., 2015, 2016) have been established through the lidar network. System alignment is one of the fundamental setup tests because the partial overlap between the laser beam and the receiver field of view has a substantial impact on lidar measurements of particle optical characteristics (Freudenthaler et al., 2018). The fact that the ray bundles from various telescopic aperture regions go through the optical setup

in various ways and with various incidence angles on the optical components can be used to assess the lidar system alignment i.e., full overlap between laser beam and telescope field of view. It is necessary to do a series of measurements using a telescope that is only partially covered so that each measurement actually represents the collection of backscattered light by a specific sector of the telescope in order to evaluate the alignment. Following the procedure described in Freudenthaler et al. (2018), a version of so-called telecover test using the set up of the telescope with four sectors was conducted in this study. For the fine alignment of the system in the far field, the range-corrected lidar signal is compared to the attenuated Rayleigh backscatter coefficient at a range interval which is considered aerosol free. To determine the lidar signal distortions due to the electronic noise the so-called dark measurement was performed. Dark signal was measured with fully covered telescope so that no light from the atmosphere and laser backscattered pulses could be detected. The lidar signals were preprocessed taking into the account 3 min dark signal (for both analog and photon counting channels) corresponding to 3600 laser shots. Such temporal averaged dark measurement with sufficient signal-to-noise ratio was subtracted from the lidar signals to improve the accuracy. In addition, experimental verification of the zero range of the signal detection was conducted (Barbosa et al., 2014).

3. Results and Discussion

3.1. Zero bin test

A trigger-delay between the actual laser pulse emission and the backscatter signal recording's presumed zero range (zero bin) can introduce notable inaccuracies in the near range signal. Particularly, the inversion of Raman signals can be significantly distorted since the signal slope in the near range varies considerably when the zero bin for range correction is changed (Freudenthaler et al., 2018). The signal peaks obtained from light reflected from a diffuse scattering target placed right above the emission part of the lidar system in order to block the laser path are presented in Figure 1. In order to prevent signal saturation the telescope was covered so that only a portion of the diffused light can enter the telescope. The first bin of the signal peak is the assessed zero bin. Since the analog to photon counting (AN-PC) signal delay might be different among LICEL transient recorder modules, the AN-PC delay should be further calculated for each module separately. In this paper the cross-correlation of the two range corrected signals was used to calculate the analog-pc delay (Barbosa et al., 2014). Analysis of the relative delay between zero-bin-corrected analog RCS and the PC RCS signals is presented in Figure 2 with the same system alignment as in Figure 3. For measurement of this delay, 30 profiles of 1200 shots each were used. A linear regression between AN and PC data was performed as a function of time delay from -10 to 10 bins. A distinct peak at -2 relative delay bins is clearly exhibited for elastic channel (with respect to zero-bin-corrected

AN signal). The main peaks for relative delay in the case of Raman channel are distributed between two range-bins, but the best assessment for relative delay corresponds also to -2 bins.

3.2. Telecover test

To check the laser-telescope alignment the telecover test using quarters of the telescope was used. This quadrant test used four sectors named North (N)-oriented from the telescope optical axis towards the laser optical axis, East (E), West (W) and South (S). The North2 (N2) signals were acquired using the same telecover sector as the N signals, but at the end of the measurement time sequence, thus deviations in the N and N2 signals reveal the effect of the changing environment during the measurements. Figure 3 and Figure 4 show relative deviations of signals collected with quadrant telescope sectors under stable atmospheric conditions on April 27, 2020 for both 355 nm and 387 nm channels, respectively. Signals obtained with a partly covered telescope are examined in terms of each sector deviation relative to the average of all signals in order to verify lidar response in the near field. The threshold for the accepted relative deviation of each sector signal is adopted to be 0.05. From the obtained results it can be seen that the Raman lidar response in the near field is below threshold and well alligned starting from 300 m. Although the telecover test is useful for the assessment of the far range response of the lidar system usually the additional test called Rayleigh fit should be applied.

3.3. Rayleigh fit test

To test the lidar alignment in the far range the Rayleigh fit procedure was used. For that purpose, the fitting of normalized lidar signal to the calculated attenuated Rayleigh backscatter coefficient (β_m^{attn}) in a range where we assume clean conditions (aerosol-free atmosphere) was performed. In Figure 5 and Figure 6 Rayleigh fit and corresponding relative deviations from the calculated Rayleigh signal for the elastic 355 nm and Raman 387 nm channels are presented. The 30 min measurements were performed during the night on the same day and with the lidar setup as presented in Figure 3. Molecular signals were calculated from the obtained Global Data Assimilation System (GDAS) profiles for the same day at 23UT following Bucholtz (1995)(Bucholtz, 1995). From Figure 5 it can be seen that the lidar system is well aligned up to the 14 km for elastic channel with the relative error less than 1% of the attenuated Rayleigh backscatter signal while Raman channel signal to noise ratio is acceptable up to the 8 km. Once the system is properly aligned it can be used for systematic aerosol measurements.

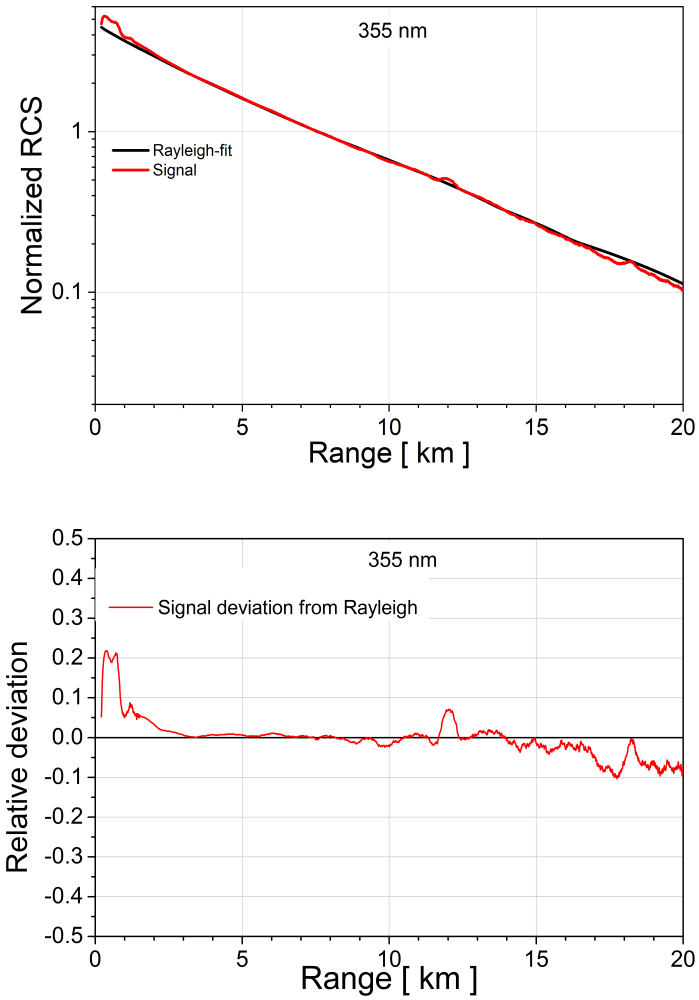

Figure 5. Photon counting 355 nm lidar signal (red) averaged over 30 minutes and calculated Rayleigh signal (black) from local radiosonde data of the same night, both normalised between 5 and 10 km range (above). Relative deviation from the calculated Rayleigh signal (below).

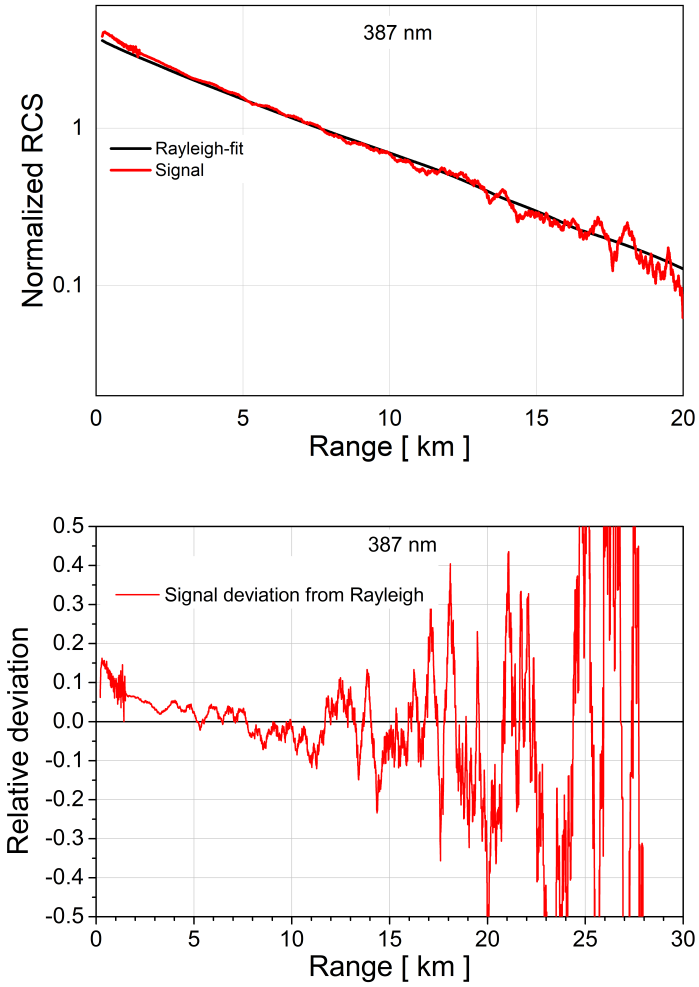

Figure 6. Photon counting 387 nm lidar signal (red) averaged over 30 minutes and calculated Rayleigh signal (black) from local radiosonde data of the same night, both normalised between 5 and 10 km range (above). Relative deviation from the calculated Rayleigh signal (below).

4. Summary

Lidar systems are optimal tools for providing range-resolved aerosol optical parameters and information on the atmospheric structure not only for climatological purposes but also in emergency situations when near real time delivery of the data and fast data processing is required. Although several lidar instrument

intercomparison campaigns have been conducted within the network, it is not possible to evaluate all systems in their specific setup due to the constant technological development and subsequently systems upgrade together with improving measurements experiences. To overcome limited capacity for providing direct intercomparisons a complementary quality-assurance procedures and tools have been developed for regular internal system check-ups across the lidar network. In this paper the capabilities of the Belgrade Raman lidar system is assessed and characterization related to zero bin assessment, analog to photon-counting signal delay, Rayleigh-fit and telecover tests to evaluate system accuracy, are presented. Under described system setup the full overlap of the telescope field of view and laser beam is measured and the system alignment is assessed in the near field starting from 300 m. In the far range the Rayleigh fit procedure for elastic 355 nm channel exhibited good signal to noise ratio and alignment up to 14 km, but Raman channel at 387 nm demonstrated significant signal noise above 8 km. In addition, the cross correlation of the two range corrected analog and photon count signals was used to assess the analog-pc delay characteristic for each transient record module.

As a unique system in the region capable to perform remote monitoring of atmospheric aerosols it is expected to perform systematic measurements on a regular schedule in the near future and contribute to the collection of aerosol vertical distribution database in Europe. Lidar measurements of aerosol optical properties can be used for model evaluation (Meier et al., 2012; Binietoglou et al., 2015). Furthermore, the assimilation of lidar observations of aerosol vertical distribution (Cheng et al., 2019) can improve model estimation of aerosol impact on climate. In addition, changes in atmospheric properties caused by specific events, like solar eclipse-induced planetary boundary layer height changes or airborne particles transport can be observed. Having in mind geographical distribution of currently active lidar stations in Europe, Belgrade Raman lidar station can provide valuable data for intercomparison and validation of optical products for future satellite missions, but automatization of the measurement process and the upgrade to the multiwavelength lidar system are essential to develop in the future.

Acknowledgements. The authors acknowledge funding provided by the Institute of Physics Belgrade, through the grant by the Ministry of Science, Technological Development and Innovations of the Republic of Serbia. The financial support for EARLINET in the ACTRIS Research Infrastructure Project by the European Union's Horizon 2020 research and innovation programme under grant agreement No. 654109 and previously under the grants No. 262254 in the 7th Framework Programme (FP7/2007-2013) is gratefully acknowledged.

References

Abril-Gago, J., Guerrero-Rascado, J. L., Costa, M. J., et al., Statistical validation of Aeolus L2A particle backscatter coefficient retrievals over ACTRIS/EARLINET stations on the Iberian Peninsula. 2022, *Atmospheric Chemistry and Physics*, **22**, 1425, DOI: 10.5194/acp-22-1425-2022

Amiridis, V., Melas, D., Balis, D. S., et al., Aerosol Lidar observations and model calculations of the Planetary Boundary Layer evolution over Greece, during the March 2006 Total Solar Eclipse. 2007, *Atmospheric Chemistry and Physics*, **7**, 6181, DOI: 10.5194/acp-7-6181-2007

Aplin, K. & Harrison, R., Meteorological effects of the eclipse of 11 August 1999 in cloudy and clear conditions. 2003, *Proceedings of the Royal Society of London. Series A: Mathematical, Physical and Engineering Sciences*, **459**, 353, DOI: 10.1098/rspa.2002.1042

Barbosa, H. M. J., Barja, B., Pauliquevis, T., et al., A permanent Raman lidar station in the Amazon: description, characterization, and first results. 2014, *Atmospheric Measurement Techniques*, **7**, 1745, DOI: 10.5194/amt-7-1745-2014

Binietoglou, I., Basart, S., Alados-Arboledas, L., et al., A methodology for investigating dust model performance using synergistic EARLINET/AERONET dust concentration retrievals. 2015, *Atmospheric Measurement Techniques*, **8**, 3577, DOI: 10.5194/amt-8-3577-2015

Boucher, O., Randall, D., Artaxo, P., et al. 2013, *Clouds and aerosols* (Cambridge, UK: Cambridge University Press), 571–657

Bucholtz, A., Rayleigh-scattering calculations for the terrestrial atmosphere. 1995, *Appl. Opt.*, **34**, 2765, DOI: 10.1364/AO.34.002765

Cheng, Y., Dai, T., Goto, D., et al., Investigating the assimilation of CALIPSO global aerosol vertical observations using a four-dimensional ensemble Kalman filter. 2019, *Atmospheric Chemistry and Physics*, **19**, 13445, DOI: 10.5194/acp-19-13445-2019

D'Amico, G., Amodeo, A., Baars, H., et al., EARLINET Single Calculus Chain – overview on methodology and strategy. 2015, *Atmospheric Measurement Techniques*, **8**, 4891, DOI: 10.5194/amt-8-4891-2015

D'Amico, G., Amodeo, A., Mattis, I., Freudenthaler, V., & Pappalardo, G., EARLINET Single Calculus Chain – technical – Part 1: Pre-processing of raw lidar data. 2016, *Atmospheric Measurement Techniques*, **9**, 491, DOI: 10.5194/amt-9-491-2016

Freudenthaler, V., Linné, H., Chaikovski, A., Rabus, D., & Groß, S., EARLINET lidar quality assurance tools. 2018, *Atmospheric Measurement Techniques Discussions*, **2018**, 1, DOI: 10.5194/amt-2017-395

Ilić, L., Kuzmanoski, M., Kolarž, P., et al., Changes of atmospheric properties over Belgrade, observed using remote sensing and in situ methods during the partial solar eclipse of 20 March 2015. 2018, *Journal of Atmospheric and Solar-Terrestrial Physics*, **171**, 250, DOI: https://doi.org/10.1016/j.jastp.2017.10.001, vertical Coupling in the Atmosphere-Ionosphere System: Recent Progress

Illingworth, A. J., Barker, H. W., Beljaars, A., et al., The EarthCARE Satellite: The Next Step Forward in Global Measurements of Clouds, Aerosols, Precipitation, and Radiation. 2015, *Bulletin of the American Meteorological Society*, **96**, 1311 , DOI: https://doi.org/10.1175/BAMS-D-12-00227.1

Kolarž, P., Šekarić, J., Marinković, B., & Filipović, D., Correlation between some of the meteorological parameters measured during the partial solar eclipse, 11 August 1999. 2005, *Journal of Atmospheric and Solar-Terrestrial Physics*, **67**, 1357, DOI: https://doi.org/10.1016/j.jastp.2005.07.016

Kolev, N., Tatarov, B., Grigorieva, V., et al., Aerosol Lidar and in situ ozone observations of the planetary boundary layer over Bulgaria during the solar eclipse of 11 August 1999. 2005, *International Journal of Remote Sensing*, **26**, 3567, DOI: 10.1080/01431160500076939

Mattis, I., D'Amico, G., Baars, H., et al., EARLINET Single Calculus Chain - technical - Part 2: Calculation of optical products. 2016, *Atmospheric Measurement Techniques*, **9**, 3009, DOI: 10.5194/amt-9-3009-2016

Maurya, A. K., Phanikumar, D. V., Singh, R., et al., Low-mid latitude D region ionospheric perturbations associated with 22 July 2009 total solar eclipse: Wave-like signatures inferred from VLF observations. 2014, *Journal of Geophysical Research: Space Physics*, **119**, 8512, DOI: https://doi.org/10.1002/2013JA019521

Meier, J., Tegen, I., Mattis, I., et al., A regional model of European aerosol transport: Evaluation with sun photometer, lidar and air quality data. 2012, *Atmospheric Environment*, **47**, 519, DOI: https://doi.org/10.1016/j.atmosenv.2011.09.029

Nymphas, E., Adeniyi, M., Ayoola, M., & Oladiran, E., Micrometeorological measurements in Nigeria during the total solar eclipse of 29 March, 2006. 2009, *Journal of Atmospheric and Solar-Terrestrial Physics*, **71**, 1245, DOI: https://doi.org/10.1016/j.jastp.2009.04.014

Papagiannopoulos, N., D'Amico, G., Gialitaki, A., et al., An EARLINET early warning system for atmospheric aerosol aviation hazards. 2020, *Atmospheric Chemistry and Physics*, **20**, 10775, DOI: 10.5194/acp-20-10775-2020

Pappalardo, G., Amodeo, A., Apituley, A., et al., EARLINET: towards an advanced sustainable European aerosol lidar network. 2014, *Atmospheric Measurement Techniques*, **7**, 2389, DOI: 10.5194/amt-7-2389-2014

Stocker, T. F., Qin, D., Plattner, G.-K., et al. 2013, *Technical summary* (Cambridge, UK: Cambridge University Press), 33–115

Wandinger, U., Freudenthaler, V., Baars, H., et al., EARLINET instrument intercomparison campaigns: overview on strategy and results. 2016, *Atmospheric Measurement Techniques*, **9**, 1001, DOI: 10.5194/amt-9-1001-2016